

Quadrupole interactions: NMR, NQR, and in between from a single viewpoint

Alex D. Bain*

Nuclear spins with quantum numbers $>1/2$ can interact with a static magnetic field, or a local electric field gradient, to produce quantized energy levels. If the magnetic field interaction dominates, we are doing nuclear magnetic resonance (NMR). If the interaction of the nuclear electric quadrupole with electric field gradients is much stronger, this is nuclear quadrupole resonance (NQR). The two are extremes of a continuum, as the ratio of one interaction to the other changes. In this work, we look at this continuum from a single, unified viewpoint based on a Liouville-space approach: the direct method. This method does not require explicit operators and their commutators, unlike Hamiltonian methods. We derive both the quadrupole-perturbed NMR solution and also the Zeeman-perturbed NQR results. Furthermore, we examine the polarization of these signals, because this is different between pure NMR and pure NQR spectroscopy. Spin 3/2 is the focus here, but the approach is perfectly general and can be applied to any spin. Copyright © 2016 John Wiley & Sons, Ltd.

Keywords: NMR; NQR; perturbation theory; quadrupolar interaction; direct method; spherical tensors; Liouvillian

Introduction

The quadrupolar interaction is the only common spin phenomenon that can rival the strength of the Zeeman interaction of the spin with an external magnetic field. If the Zeeman interaction dominates, we are doing nuclear magnetic resonance (NMR) and can usually treat the quadrupole interaction with perturbation theory.^[1–5] In zero field, the nuclear quadrupole moment interacts with the local electric field gradient to give quantized spin energy levels. If we observe transitions between these levels, this is nuclear quadrupole resonance (NQR) spectroscopy.^[6,7] This spectroscopy becomes much richer if a small external magnetic field is applied, and these effects can also be treated by perturbation theory.^[6] NMR and NQR have tended to develop separately, but our aim in this paper is to try to treat them both with a common approach.

One important reason for this study is that systems with larger and larger quadrupolar interactions are being studied, which test the limits of perturbation theory.^[8,9] If we can tie down the ends of the NMR–NQR continuum with the same formalism, then this helps us in the more complicated intermediate region. The ordering of the spin states is quite different in zero and high field (Fig. 1), so the intermediate region is bound to be interesting.^[10–12]

One aspect is deciding roughly where the spectroscopy changes from 'NQR-like' to 'NMR-like'. Numerical solutions may well be necessary and are readily available, but analytical formulae can be helpful in interpreting them.

There is also some interesting spectroscopy here, because NMR signals are circularly polarized, but pure NQR signals are linearly polarized. If a cross-coil probe is used to observe NQR, for certain relative orientations of the two coils, no signal will be observed.^[6,7,13,14] This raises the question of what happens between those extremes. If we use a single-coil probe, these effects may not be observed, but polarization could be a useful observable.

Polarization is a central concept in electromagnetic radiation and plays an important role in several forms of spectroscopy. The electric and magnetic fields associated with the radiation are

perpendicular to the direction of propagation, and the trajectories of these fields can be thought of in two equivalent ways. One is linear polarization, in which the fields oscillate but remain in one plane, and the other is circular polarization, in which the fields follow a helical path. The two are equivalent, because we can form a helix from the x and y components, or we can create linear polarization by combining two counter-rotating helices. Details of how polarization affects NQR were studied long ago^[15] and have been applied to the spin-1 case^[16,17] and numerical simulations (using the Hamiltonian approach) of quantum computing.^[18] Because we use radiofrequency (RF) radiation to manipulate and observe spin resonance, it is important to consider the role of polarization.

The polarization of the signals we discuss is a relative measurement, comparing the phase of the input excitation RF to that of the signals that are emitted. This is best observed when the transmitter and the detection coils in the probe are separate. In almost all modern spectrometers, a single coil is used for both roles, so we are much less aware of polarization, and it has little effect on our experiment. In a pulse sequence, the relative phases of the various pulses play a vital role, but these phases are all within the excitation side of the spectrometer. We only detect the signal at the end of the pulse sequence. It is the polarization of the output signal relative to the excitation that concerns us here.

In this paper we concentrate of the spin-3/2 system with Zeeman and quadrupole interaction. Because this Liouvillian is a 15×15 matrix, this is an easy system to deal with, but the approach is completely general and can be applied to any spin. Although some of the results here are already in the literature, we propose an approach that produces new insights.

* Correspondence to: Alex D. Bain, Department of Chemistry and Chemical Biology, McMaster University, 1280 Main St. West, Hamilton, Ontario, L8S 4M1, Canada. E-mail: bain@mcmaster.ca

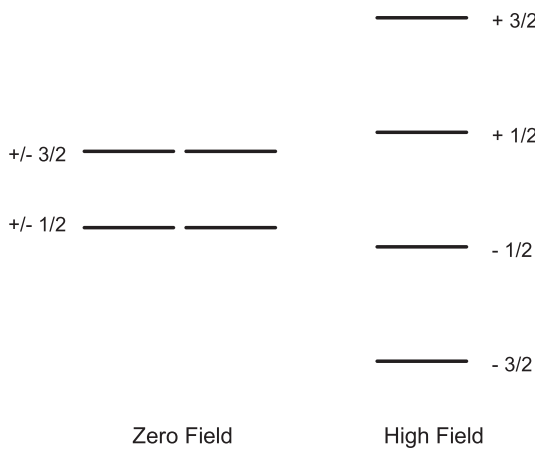


Figure 1. Energy levels of a spin-3/2 with a quadrupole coupling in zero magnetic field (left) and high magnetic field (right). The quantum numbers give the z component of the nuclear spin.

Theoretical Background

The direct method^[19–21] is the way that we will analyze the perturbations in both NMR and NQR. This is well-established in magnetic resonance and has been recently included in a wider context.^[22] In this technique, we deal directly with the transitions (coherences) without having to use Hamiltonians first to calculate the wave functions. The important operator here is now the Liouvillian,^[23] which can be derived from the Hamiltonian, but it can also be calculated directly. Diagonalization of the Hamiltonian matrix gives us the wavefunctions and their energies, from which we can construct the observable transitions. Diagonalization of the Liouvillian gives us the transitions and their frequencies directly, without the intermediate step of the wavefunctions.

Modern NMR is usually concerned with the time evolution of the spin system. This is governed by the Liouville-von Neumann equation. In Hilbert space (the Hamiltonian approach), the equation of motion of the density matrix is given by Eqn (1)

$$\frac{d}{dt}\hat{\rho} = -i \left[\hat{H}, \hat{\rho} \right], \quad (1)$$

where $\hat{\rho}$ is the density matrix and \hat{H} is the Hamiltonian operator. Note that we have put hats on the symbols to indicate that they represent operators in Hilbert space. The core of this calculation is the evaluation of the operator commutators, which requires a detailed knowledge of the operators.

In the direct, Liouville-space methods, the time evolution is written as in Eqn (2)

$$\frac{d}{dt}\rho = -i L\rho, \quad (2)$$

where L is the Liouvillian. This is a superoperator in Hilbert space,^[20] but a standard operator (or matrix) in Liouville space. The density matrix, ρ , has no hat here, because it is a vector in Liouville space. Because both approaches must give the same answer, this change from Hilbert space to Liouville space is partly a change of notation. However, the Liouville space method offers some significant advantages.

No commutators or details of the operators are needed^[21] in this approach, provided we use a spherical tensor basis. This prompts a deviation from the standard notation for spherical tensor

operators^[24–29] and the density matrix. The usual notation for a spherical tensor is of the form T_q^n , where n and q are the rank and order of the spherical tensors.^[25] Because these two quantum numbers are all we need, we can dispense with the T and write the spherical tensor operator as a Liouville-space ket (with round brackets), in direct imitation of the way that spin wave functions are written as kets (with angle brackets) containing just the quantum numbers. Refer to Table 1 for some examples.

Single transition operators^[30] offer an alternative approach, and they work well for treating single transitions. However, for the full system, this approach produces an overcomplete basis – if you use all the transitions, there are more operators than the linearly independent set, so constraints must be imposed. Because we are dealing with the whole system here, we feel that spherical tensors are the best way.

Another simplification is the identification of observable quantities. With operators, this is performed by taking the trace of the product of density matrix and the operator representing the observable – usually I_x or I_+ . In Liouville space, the inner, or dot, product between two vectors is defined as the trace of the product of the corresponding operators. We usually make I_+ one of the elements of the basis set (Table 1) – it is many ways the simplest. Therefore, the observable value, $\langle I_+ \rangle$, is just the element of the density matrix that matches I_+ in the basis set. Simple!

The explicit formula for any commutator is provided by angular momentum theory, in particular, formulae for the products of tensor operators.^[31,32] With only the quantum numbers of the spherical tensor basis, we can calculate all the matrix elements of the spin Liouvillian from a set of formulae.^[21,33] This is reminiscent of the calculation of Hamiltonian matrix elements. To set up the Hamiltonian, we know nothing of the spin wavefunctions beyond their quantum numbers, which we then substitute into established formulae. Although we have all the details of the basis operators, they are not needed. All that is required is the quantum numbers to be used in the formulae.

Tables 2–4 give the full Liouvillian for a spin 3/2 with a quadrupole interaction and magnetic fields. Figure 1 shows the energy levels for the NMR and NQR extreme cases. There are no

Table 1. Examples of the notation used in this paper and its comparison to more standard notations for some of the spin-3/2 spherical tensors

$ 0\rangle$	T_0^0	$\frac{1}{2}T_0^0$	$\frac{1}{2}I_1$	unit
$ 1_{+1}\rangle$	T_{+1}^1	$\frac{1}{\sqrt{5}}T_{+1}^1$	$-\frac{1}{\sqrt{10}}I_+$	$-\frac{1}{\sqrt{10}}(I_x + i, I_y)$
$ 1_0\rangle$	T_0^1	$\frac{1}{\sqrt{5}}T_0^1$	$\frac{1}{\sqrt{5}}I_z$	$\frac{1}{\sqrt{5}}I_z$
$ 1_{-1}\rangle$	T_{-1}^1	$\frac{1}{\sqrt{5}}T_{-1}^1$	$\frac{1}{\sqrt{10}}I_-$	$\frac{1}{\sqrt{10}}(I_x - i, I_y)$

Full expressions for all the spin-3/2 operators have been published elsewhere.^[21] The first column shows the notation used in this paper, and the second and third columns show the normalized and unnormalized spherical tensors from Bowden *et al.*^[26] The final two columns on the right show the operator forms of the spherical tensors. Note that the forms of the operators are the same for all spins, but the normalization constant will change with the total spin quantum number.

approximations used in setting this up, so this Liouvillian covers NMR, NQR, and all the intermediate cases. We apply approximations to get the analytical perturbation solutions, but the Liouvillian itself is perfectly general.

Nuclear Magnetic Resonance

The helicity of signals in NMR is already familiar. In looking at the effect of RF radiation, we usually use a rotating frame of reference – we choose one sense and ignore the counter-rotating component. The photon carries a spin of 1, so absorption or emission will change the spin quantum number by ± 1 . For instance, circularly polarized light is the source of sensitivity enhancement in noble gas-based hyperpolarization. In a coherence pathway diagram, the coherence level of a signal has a sign associated with it, which is a fundamental concept. The positive and negative signs can be considered as representing the two senses of helicity.

In NMR, the net magnetization precesses in a single direction, because it starts along z and is flipped into the xy plane. The direction will depend on the sign of the magnetogyric ratio. However, there is no inherent helicity in the signal we detect, because there is a single receiver coil and only one wire which comes out of the probe. Two orthogonal coils have been used in imaging contexts,^[34] but this turns out to offer few real advantages in NMR. In the receiver we introduce polarization when we do quadrature detection^[35] by mixing the signal with two RF signals that are $\pi/2$ out of phase. The sign of the helicity is determined by the sign of the phase difference.

Table 3. The next three columns of the Liouvillian matrix for a spin 3/2 experiencing the Zeeman, quadrupole, and RF interaction

Columns 7–9

Basis elements: $|3_0\rangle |2_0\rangle |1_0\rangle$

$$\begin{bmatrix} 0 & 0 & 0 \\ 0 & \sqrt{2}\sqrt{3}V_{+2} & 0 \\ -\frac{1}{5}\sqrt{2}\sqrt{5}\sqrt{3}V_{+2} & 0 & \frac{2}{5}\sqrt{30}V_{+2} \\ 2\sqrt{3}B_1 & -\frac{2}{5}\sqrt{5}\sqrt{3}V_{+1} & 0 \\ -\frac{2}{5}\sqrt{2}\sqrt{5}\sqrt{3}V_{+1} & \sqrt{6}B_1 & -\frac{1}{5}\sqrt{30}V_{+1} \\ 0 & -\frac{3}{5}\sqrt{10}V_{+1} & \sqrt{2}B_1 \\ 0 & 0 & 0 \\ 0 & 0 & 0 \\ 0 & 0 & 0 \\ 2\sqrt{3}B_1 & \frac{2}{5}\sqrt{5}\sqrt{3}V_{-1} & 0 \\ \frac{2}{5}\sqrt{2}\sqrt{5}\sqrt{3}V_{-1} & \sqrt{6}B_1 & \frac{1}{5}\sqrt{30}V_{-1} \\ 0 & \frac{3}{5}\sqrt{10}V_{-1} & \sqrt{2}B_1 \\ 0 & -\sqrt{2}\sqrt{3}V_{-2} & 0 \\ \frac{1}{5}\sqrt{2}\sqrt{5}\sqrt{3}V_{-2} & 0 & -\frac{2}{5}\sqrt{30}V_{-2} \\ 0 & 0 & 0 \end{bmatrix}$$

These have a resonance frequency of zero in a magnetic field and correspond to the z magnetizations in the absence of quadrupole coupling.

Table 2. The first six columns of the 15×15 Liouvillian matrix for a spin 3/2 experiencing the Zeeman, quadrupole, and RF interaction

Columns 1–6

Basis elements: $|3_{+3}\rangle |3_{+2}\rangle |2_{+2}\rangle |3_{+1}\rangle |2_{+1}\rangle |1_{+1}\rangle$

$$\begin{bmatrix} 3\gamma B_0 & \sqrt{6}B_1 & \sqrt{2}\sqrt{3}V_{+1} & 0 & \sqrt{2}\sqrt{3}V_{+2} & 0 \\ \sqrt{6}B_1 & 2\gamma B_0 & -\sqrt{2}\sqrt{3}V_0 & \sqrt{10}B_1 & 0 & 0 \\ -\sqrt{2}\sqrt{3}V_{-1} & -\sqrt{2}\sqrt{3}V_0 & 2\gamma B_0 & -\frac{3}{5}\sqrt{2}\sqrt{5}V_{+1} & 2B_1 & \frac{2}{5}\sqrt{15}V_{+1} \\ 0 & \sqrt{10}B_1 & \frac{3}{5}\sqrt{2}\sqrt{5}V_{-1} & \gamma B_0 & -\frac{2}{5}\sqrt{5}\sqrt{3}V_0 & 0 \\ \sqrt{2}\sqrt{3}V_{-2} & 0 & 2B_1 & -\frac{2}{5}\sqrt{5}\sqrt{3}V_0 & \gamma B_0 & -\frac{3}{5}\sqrt{10}V_0 \\ 0 & 0 & -\frac{2}{5}\sqrt{15}V_{-1} & 0 & -\frac{3}{5}\sqrt{10}V_0 & \gamma B_0 \\ 0 & 0 & -\frac{1}{5}\sqrt{2}\sqrt{5}\sqrt{3}V_{-2} & 2\sqrt{3}B_1 & \frac{2}{5}\sqrt{2}\sqrt{5}\sqrt{3}V_{-1} & 0 \\ 0 & \sqrt{2}\sqrt{3}V_{-2} & 0 & \frac{2}{5}\sqrt{5}\sqrt{3}V_{-1} & \sqrt{6}B_1 & \frac{3}{5}\sqrt{10}V_{-1} \\ 0 & 0 & \frac{2}{5}\sqrt{30}V_{-2} & 0 & \frac{1}{5}\sqrt{30}V_{-1} & \sqrt{2}B_1 \\ 0 & 0 & 0 & 0 & -\frac{3}{5}\sqrt{2}\sqrt{5}V_{-2} & 0 \\ 0 & 0 & 0 & \frac{3}{5}\sqrt{2}\sqrt{5}V_{-2} & 0 & -\frac{2}{5}\sqrt{15}V_{-2} \\ 0 & 0 & 0 & 0 & \frac{2}{5}\sqrt{15}V_{-2} & 0 \\ 0 & 0 & 0 & 0 & 0 & 0 \\ 0 & 0 & 0 & 0 & 0 & 0 \end{bmatrix}$$

These correspond to transitions with a positive NMR frequency. The elements down the main diagonal are the Zeeman terms, proportional to γB_0 , where γ is the magnetogyric ratio and B_0 is the static magnetic field. The terms in B_1 represent the interaction with the RF magnetic field. The quadrupole terms have a spin part, given in the table, multiplied by a spatial term denoted by V_n where n runs from -2 to $+2$. The V_n terms are defined at the end of Table 4. The basis elements for this matrix are spherical tensor operators, denoted as $|M_n\rangle$, and the basis elements corresponding to the columns are given at the top. This notation deviates from the standard T -based notation for spherical tensors,^[24,26] because it retains only the quantum numbers corresponding to the rank and order. We do this deliberately because the operator character, although known, is not needed here: the quantum numbers suffice. The details of the notation and its relation to standard operators has been published.^[21]

Table 4. The last six columns of the Liouvillian matrix for a spin 3/2 experiencing the Zeeman, quadrupole, and RF interaction

Columns 10–15

Basis elements: $|3_{-1}\rangle |2_{-1}\rangle |1_{-1}\rangle |3_{-2}\rangle |2_{-2}\rangle |3_{-3}\rangle$

$$\begin{bmatrix} 0 & 0 & 0 & 0 & 0 & 0 \\ 0 & 0 & 0 & 0 & 0 & 0 \\ 0 & 0 & 0 & 0 & 0 & 0 \\ 0 & \frac{3}{5}\sqrt{2}\sqrt{5}V_{+2} & 0 & 0 & 0 & 0 \\ -\frac{3}{5}\sqrt{2}\sqrt{5}V_{+2} & 0 & \frac{2}{5}\sqrt{15}V_{+2} & 0 & 0 & 0 \\ 0 & -\frac{2}{5}\sqrt{15}V_{+2} & 0 & 0 & 0 & 0 \\ 2\sqrt{3}B_1 & -\frac{2}{5}\sqrt{2}\sqrt{5}\sqrt{3}V_{+1} & 0 & 0 & \frac{1}{5}\sqrt{2}\sqrt{5}\sqrt{3}V_{+2} & 0 \\ -\frac{2}{5}\sqrt{5}\sqrt{3}V_{+1} & \sqrt{6}B_1 & -\frac{3}{5}\sqrt{10}V_{+1} & -\sqrt{2}\sqrt{3}V_{+2} & 0 & 0 \\ 0 & -\frac{1}{5}\sqrt{30}V_{+1} & \sqrt{2}B_1 & 0 & -\frac{2}{5}\sqrt{30}V_{+2} & 0 \\ -\gamma B_0 & \frac{2}{5}\sqrt{5}\sqrt{3}V_0 & 0 & \sqrt{10}B_1 & -\frac{3}{5}\sqrt{2}\sqrt{5}V_{+1} & 0 \\ \frac{2}{5}\sqrt{5}\sqrt{3}V_0 & -\gamma B_0 & \frac{3}{5}\sqrt{10}V_0 & 0 & 2B_1 & -\sqrt{2}\sqrt{3}V_{+2} \\ 0 & \frac{3}{5}\sqrt{10}V_0 & -\gamma B_0 & 0 & \frac{2}{5}\sqrt{15}V_{+1} & 0 \\ \sqrt{10}B_1 & 0 & 0 & -2\gamma B_0 & \sqrt{2}\sqrt{3}V_0 & \sqrt{6}B_1 \\ \frac{3}{5}\sqrt{2}\sqrt{5}V_{-1} & 2B_1 & -\frac{2}{5}\sqrt{15}V_{-1} & \sqrt{2}\sqrt{3}V_0 & -2\gamma B_0 & \sqrt{2}\sqrt{3}V_{+1} \\ 0 & -\sqrt{2}\sqrt{3}V_{-2} & 0 & \sqrt{6}B_1 & -\sqrt{2}\sqrt{3}V_{-1} & -3\gamma B_0 \end{bmatrix}$$

$$V_{+2} = -\frac{1}{24}e^2qQ(\eta \cos(2\varphi) + 2i\eta \cos(\theta)\sin(2\varphi) + \eta(\cos(\theta))^2\cos(2\varphi) - 3 + 3(\cos(\theta))^2)$$

$$V_{+1} = \frac{1}{12}\sin(\theta)e^2qQ(i\eta \sin(2\varphi) + \eta \cos(\theta)\cos(2\varphi) + 3\cos(\theta))$$

$$V_0 = \frac{1}{24}e^2qQ\sqrt{6}(-\eta \cos(2\varphi) + \eta(\cos(\theta))^2\cos(2\varphi) + 3(\cos(\theta))^2 - 1)$$

$$V_{-1} = -\frac{1}{12}\sin(\theta)e^2qQ(-i\eta \sin(2\varphi) + \eta \cos(\theta)\cos(2\varphi) + 3\cos(\theta))$$

$$V_{-2} = -\frac{1}{24}e^2qQ(\eta \cos(2\varphi) - 2i\eta \cos(\theta)\sin(2\varphi) + \eta(\cos(\theta))^2\cos(2\varphi) - 3 + 3(\cos(\theta))^2)$$

These are the negative-frequency counterparts of the element in Table 1. The quadrupole interaction is defined in the usual way^[1,3–5] via a coupling constant, e^2qQ and an asymmetry parameter, η . The orientation of the principal axes of the quadrupole tensor is given by the two angles θ and ϕ .

In the product operator method for calculating the effect of a pulse sequence,^[36–38] we use both Cartesian and spherical operators. The Cartesian operators I_x and I_y sometimes give a clearer physical picture, but they can also be combined into the raising and lowering operators, which are a form of spherical tensor operators (Table 1). The choice of what to use is arbitrary and up to the user, because they all must give the same answer. Product operators are mostly used for systems of weakly coupled spins-1/2, but for higher spins, the situation becomes more complicated. This is because there are now more operators and their commutation relationships are more complex. Because spins with strong quadrupole coupling are the only cases where polarization can be observed, we need to look at them with more general methods. We first look at the NMR of a spin 3/2 with a quadrupole perturbation.

Spin 3/2

The full Liouvillian for a single spin-3/2 with the Zeeman, quadrupole, and RF (B_1) interaction has been published^[21] and is given in Tables 2–4. If we are considering the B_1 term as RF, then it contains the $\cos(\omega t)$ time dependence. When we consider Zeeman-perturbed NQR later on, we can use the form of this term to represent the small magnetic field perturbation. This Liouvillian is a complete description which enables us to calculate the exact behavior of a spin with any sizes of the interactions. We will not need all

these capabilities, but it is useful to use them to study a spin-3/2 perturbed to second order by the quadrupole interaction (Fig. 2). Normally, this system is analyzed by looking at the perturbations of the energy levels,^[2,39] then calculating the transition energy. However, applying perturbation theory to the transitions directly^[40] has a number of advantages.

The details of how to do this have been published,^[40] so we give a quick sketch here. Figure 2 gives a schematic picture of the energy levels of the spin states for a weak quadrupole interaction. The transitions and their frequencies can be derived from this, but are more directly given by the eigenvectors and eigenvalues of the Liouvillian. Figure 3 shows all the transitions for spin 3/2. Note that in Fig. 2 the vertical scale is the energy of the levels, whereas in Fig. 3 it is the transition frequency, the difference between energy levels. The transitions are the positive and negative components of one triple-quantum transition, two double-quantum transitions, and three single-quantum transitions. The three non-redundant z magnetizations (zero coherence level) round out the 15 density matrix elements. RF terms are included in the Liouvillian, for generality but they do not concern us yet, so we set them to zero.

In the absence of the quadrupole interaction, the Liouvillian, as it is written in Tables 2–4, has only the Zeeman interaction and is already diagonal. When we discuss NQR, we will transform this Liouvillian, via a unitary transformation, to a basis in which the quadrupole interaction is diagonal. To the Zeeman-based Liouvillian we add the quadrupole interaction and treat it as a

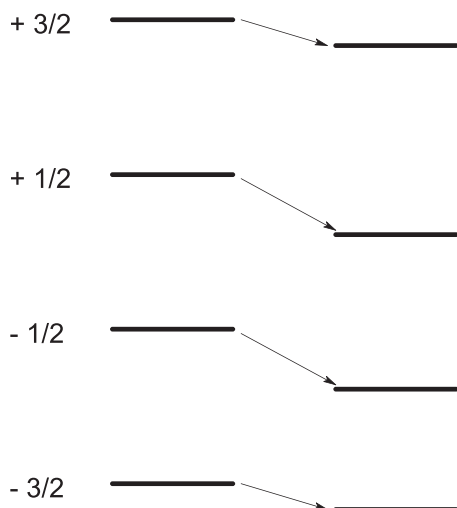


Figure 2. Energy levels of a spin-3/2 in a high magnetic field, with (right) and without (left) a small perturbing quadrupolar interaction. Without the quadrupole, the levels are equally spaced and with the quadrupole, the spacing of the $-1/2$ and $+1/2$ levels (the central transition) remains the same to first order. The spacing between the $+3/2$ and $+1/2$ levels is increased, and the other spacing is decreased to give satellite transitions equally to one side and the other of the central transition.

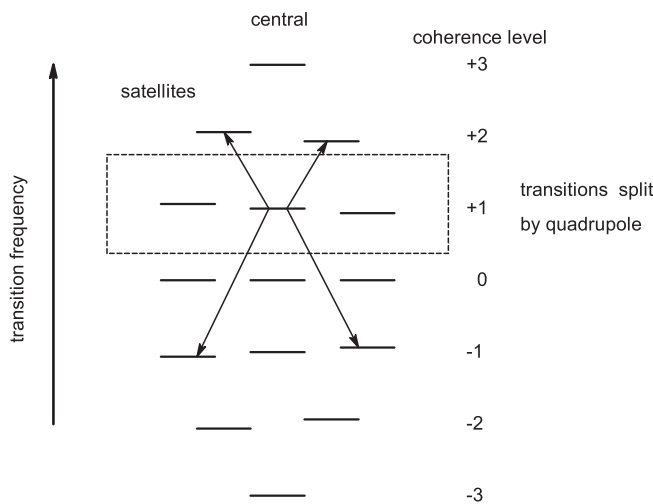


Figure 3. Schematic diagrams of all possible transitions for a spin-3/2 under a quadrupole-perturbed Zeeman interaction. There is a triple-quantum transition, two double-quantum transitions, three single-quantum transitions, and three zero-quantum transitions (level populations). There are also the negative coherence level counterparts of the triple-, double- and single-quantum transitions. The dashed box indicates the observable single-quantum transitions. Note that the y axis denotes transition frequency (difference between energies of levels) rather than the level energies shown in Figs 1 and 3. The coherence levels of the transition are shown on the right, and within a coherence level the frequencies are not the same, so the transition frequency changes from left to right. The second-order quadrupole perturbation mixes the transitions and the arrows indicate the mixing of the central transition.^[50] It is mixed specifically with the two positive double-quantum transitions and the two satellites in coherence level -1 .

perturbation.^[40] There are two steps to this process. First, the transitions within a coherence level are degenerate under just the Zeeman interaction, so the quadrupole interaction lifts that degeneracy.^[33,40] Each coherence level forms a block along the diagonal, so each of these blocks is separately diagonalized. This process gives the transitions familiar from the first-order perturbation

treatment of quadrupolar systems.^[2,39] Then the Liouvillian terms between the coherence level blocks are applied, using standard second-order perturbation theory, to give the expressions for the second-order perturbed line positions. A further result is that this shows how the transitions themselves are mixed by the perturbation. This mixing is quite specific (Fig. 3) and is governed by a number of selection rules.^[40,41] It is this mixing of the transitions that gives us a hint of the polarization changes. In particular, the transitions with a coherence level of $+1$ are mixed to a small extent with their counter-rotating partners (coherence level -1), as shown by the arrows in Fig. 3. This mixing of opposite helicities means that the polarization is no longer exactly circular.

Nuclear Quadrupole Resonance

The details of the transitions in NQR have long been known.^[6,7,42] In the absence of a magnetic field, the spin energy depends on the square of the magnetic quantum number, so $+1/2$ and $-1/2$ are degenerate, as are $\pm 3/2$ (Figs 1 and 4). The NQR spectrum of a spin-3/2 shows just a single line at a frequency of the quadrupole coupling, $C_q/2$, where C_q is given by Eqn (3)

$$C_q = \frac{e^2 q Q}{\hbar} . \quad (3)$$

A small Zeeman interaction splits the lines and (more importantly) mixes the wavefunctions with z quantum numbers of $\pm 1/2$, as shown in Fig. 4. The energies of the transitions are^[6]

$$\frac{C_q}{2} \pm \frac{3 \pm f}{2} \gamma B_1 \cos(\theta) , \quad (4)$$

where γ is the magnetoglyc ratio, B_1 (we use B_1 rather than the standard B_0 , to be consistent with Tables 2–4) is the perturbing static magnetic field at an angle θ to the principal axis of the quadrupole tensor and

$$f = \sqrt{1 + 4 \tan^2(\theta)} . \quad (5)$$

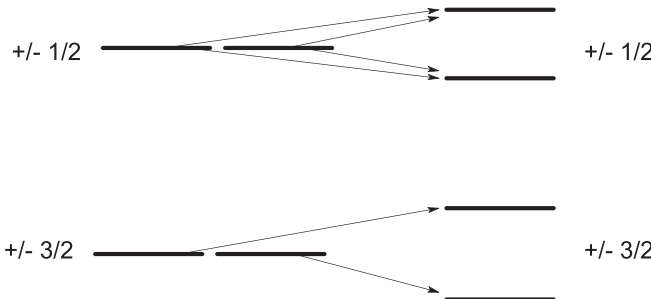


Figure 4. Energy levels of a spin-3/2 in zero magnetic field (left) and in a small perturbing magnetic field (right). The magnetic field moves the $\pm 3/2$ levels without mixing them to first order. The $\pm 1/2$ levels are both moved and mixed.

The four lines form a quartet (Fig. 5), with the following intensities

$$\begin{aligned} \text{outer} &= \frac{f-1}{2f} \\ \text{inner} &= \frac{f+1}{2f} \end{aligned} \quad . \quad (6)$$

These results were obtained by dealing with the Hamiltonian, but we can duplicate them using the direct method, to draw analogies to the NMR case.

To begin with, we remove the magnetic field terms from the Liouvillian to get the pure NQR solution. Unlike the NMR case, this Liouvillian in Tables 2–4 is not already diagonal, but calculating its symbolic eigenvalues and eigenvectors is a simple task for a computer symbolic algebra package such as Maple (www.maplesoft.com) or Mathematica (www.wolfram.com). There are four pairs of degenerate transitions at $\pm\frac{C_q}{2}$ and seven transitions with zero frequency. Three of the latter represent the z magnetizations, and the other four represent the zero-frequency transitions between degenerate levels. The matrix of eigenvectors, U_Q , forms the linear transformation, which diagonalizes the quadrupole Liouvillian.

The eigenvectors for the non-zero frequency NQR transitions are given in Eqn (7) and illustrate a number of points. These eigenvectors all have the same eigenvalue, $\frac{C_q}{2}$, and represent transitions between the energy levels $\pm\frac{1}{2}$ and $\pm\frac{3}{2}$. In this equation,

$$\begin{aligned} \frac{1}{\sqrt{2}} &\left| 3_{-2} \right\rangle + \frac{1}{\sqrt{2}} \left| 2_{-2} \right\rangle \\ \frac{1}{\sqrt{2}} &\left| 3_{+2} \right\rangle - \frac{1}{\sqrt{2}} \left| 2_{+2} \right\rangle \\ \frac{1}{\sqrt{5}} &\left| 3_{-1} \right\rangle + \frac{1}{\sqrt{2}} \left| 2_{-1} \right\rangle + \sqrt{\frac{3}{10}} \left| 1_{-1} \right\rangle \\ \frac{1}{\sqrt{5}} &\left| 3_{+1} \right\rangle - \frac{1}{\sqrt{2}} \left| 2_{+1} \right\rangle + \sqrt{\frac{3}{10}} \left| 1_{+1} \right\rangle \end{aligned} \quad . \quad (7)$$

, there are, apparently, upward and downward versions of the transitions, as can be seen from the signs of the subscripts in the basis elements, but because the quadrupole interaction depends on the square of the quantum number, the two versions are degenerate. The normal selection rules say that two are allowed and two are forbidden, and this can be seen directly in the eigenvectors. We only

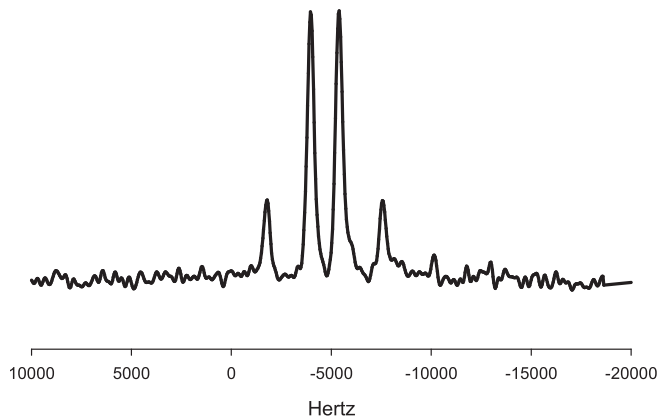


Figure 5. Nuclear quadrupole resonance (NQR) spectrum of a single crystal of KClO_3 in the stray field of an unshielded 4.7 T widebore magnet. The resonance is at approximately 18 MHz. We thank the late Hiltrud Grondorf for help in obtaining this spectrum.

detect single-quantum coherence, which is represented by the basis elements $|1_{\pm 1}\rangle$,^[23] and the transition probability for given line is the square of the overlap with the detector.^[43] Only the last two eigenvectors in Eqn (7) satisfy this, so they are the allowed transitions.

We must also define the Zeeman Liouvillian, without the quadrupole interaction, because this will serve as the perturbation. Previously, we glossed over an important point: the definition of the z axis. In NQR, this is conventionally defined by the principal axis frame of the molecule-fixed quadrupole tensor. When we apply a static magnetic field, this may or may not lie along the z axis, depending on the orientation of the molecule. The static field will have x, y, and z components. For simplicity, let us assume that the quadrupole tensor is cylindrical, so that the magnet field orientation is defined by a single angle, θ .

This definition can be accommodated in the Liouvillian in Tables 2–4. The diagonal Zeeman terms become proportional to $\gamma B_1 \cos(\theta)$. Because the RF terms in the NMR discussion, B_1 , are in the xy plane, we can replace them by the appropriate spherical tensor terms, $\frac{\gamma B_1 \sin(\theta)}{\sqrt{2}}$, derived from the static magnetic field. Once we have defined the magnetic Liouvillian, we need to transform it into the principal axis frame of the quadrupole tensor, using the matrix of eigenvectors of the quadrupole Liouvillian, U_Q .

Analogous to the NMR case, the first role of the perturbation is to raise the degeneracy of the pure NQR transitions. The quadrupole Liouvillian breaks into two 4×4 blocks, belonging to the positive and negative frequency transitions, plus a 7×7 block with zero eigenvalues, as shown schematically in Fig. 6. For these 4×4 blocks, the eigenvalues are given by Eqn (8), which is the same as the standard solution,^[6] En. (4),

$$\frac{C_q}{2} \pm \frac{3\gamma B_0}{2} \pm \frac{\gamma B_0 \sqrt{1 + 4\tan^2(\theta)}}{2} \quad . \quad (8)$$

For the 7×7 block, there are three eigenvalues that remain as zero after the perturbation, corresponding to the three unique level population differences. The other four eigenvalues are given by Eqn (9)

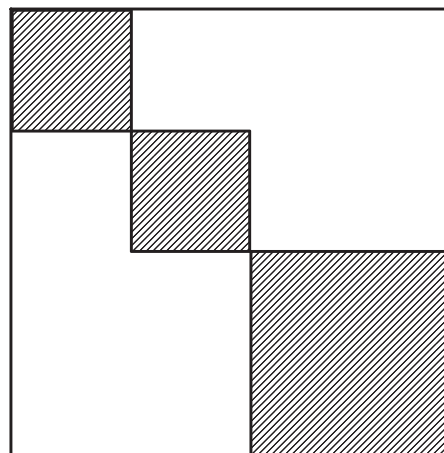


Figure 6. Schematic diagram of the structure of the 15×15 quadrupole Liouvillian matrix for a spin-3/2. Diagonalization of the Liouvillian from Tables 1–3 produces a 4×4 block with all diagonal elements of $\pm\frac{C_q}{2}$, a 4×4 block with all diagonal elements of $\mp\frac{C_q}{2}$, and a 7×7 block with zero eigenvalues. When the Zeeman perturbation is applied, it is only the terms within these blocks that are important.

$$\pm \sqrt{1 + 4\tan^2(\theta)} \quad \gamma B_0 \\ \pm 3\gamma B_0 \quad (9)$$

These represent transitions between the previously degenerate $\pm\frac{1}{2}$ and $\pm\frac{3}{2}$ spin states. As we saw in the preceding text, the $\pm\frac{1}{2}$ states are mixed, to first order, by the Zeeman perturbation, but the $\pm\frac{3}{2}$ states are not.

Note that there is an algebraic complication here, because the matrix blocks of the magnetic field Liouvillian are not symmetric. The eigenvalues are easy, because they are solutions of the characteristic equation, but the eigenvectors are more complicated.^[44,45] A similar situation arises when we deal with NMR chemical exchange in unequally populated cases.^[46,47] There is now a distinction between left and right eigenvectors, so we must be more careful.

Polarization

We observed that in the NMR case, all the transitions belonged to the +1 coherence level to first order, and it was only the second-order perturbation that mixed these with a bit of the -1 coherence level. This leads to a circularly polarized signal. If we look at the pure NQR case, Eqn (7) shows that the two observable transitions belong equally to the +1 and -1 coherence levels. Because these oscillate as $e^{+i\omega t}$ and $e^{-i\omega t}$, then their sum is linearly polarized. This can also be derived from looking at the wavefunctions to first order in the Zeeman perturbation. The unperturbed wavefunctions are $|+\frac{1}{2}\rangle$ and $|-\frac{1}{2}\rangle$, but degenerate perturbation theory says that they will mix to form the wavefunctions in Eqn (10)

$$\psi_1 = \frac{\left|+\frac{1}{2}\right\rangle + \left|-\frac{1}{2}\right\rangle}{\sqrt{2}} \\ \psi_2 = \frac{\left|+\frac{1}{2}\right\rangle - \left|-\frac{1}{2}\right\rangle}{\sqrt{2}} \quad (10)$$

A transition between these states $\psi_1 \rightarrow \psi_2$ will involve both upward $|-\frac{1}{2}\rangle \rightarrow |+\frac{1}{2}\rangle$ and downward $|+\frac{1}{2}\rangle \rightarrow |-\frac{1}{2}\rangle$ spin transitions, leading to linear polarization.

This is true only for the strict zero magnetic field case. If there is a finite perturbation, then all four transitions derived from Eqn (7) become allowed and are no longer degenerate. The cancellation from the equal mixing of opposite helicities to give linear polarization no longer applies.^[6]

A better case to look at is the comparison between the central transition in the NMR case and the transition with frequency $\sqrt{1 + 4\tan^2(\theta)} \quad \gamma B_0$ from Eqn (9). Both of these are, very roughly speaking, transitions between the Hamiltonian states $|-\frac{1}{2}\rangle \rightarrow |+\frac{1}{2}\rangle$. In the NQR extreme, this transition is a rather complicated mixture of a number of basis elements $|3_+1\rangle, |3_-1\rangle, |1_+1\rangle, |1_-1\rangle, |3_0\rangle$ and $|1_0\rangle$. Note the use of angle brackets to denote wavefunctions and the use of round brackets for Liouville-space vectors. This mixture depends on the ratio of the Zeeman to the quadrupole interaction, as do two of the z magnetizations. Again, there is an analogy to the NMR of two strongly coupled spins-1/2. In that case, the composition of the zero-quantum transition and the z magnetizations depends on the ratio of J/δ .^[48,49] In the mixture for the NQR transition with frequency $\sqrt{1 + 4\tan^2(\theta)} \quad \gamma B_0$ there is a significant

mixture of +1 and -1 coherence levels, so the line is mainly linearly polarized. These NQR results are for first-order perturbation. Because all the NQR transitions are perturbed to first order by the magnetic field, there is not much point in going to second order, even though this is a straightforward calculation, following the NMR case.

Conclusions

The single Liouvillian, given in Tables 2–4 easily reproduces all the results already in the literature and provides some new insights. The Liouvillian presented here is easily accommodated in any programming package (Matlab, Mathematica, Maple, Python, etc.) that can handle eigenvalues and eigenvectors for any specific application. In particular, it clearly shows how the polarization of the signals changes as the relative strengths of the Zeeman and quadrupole interaction change. At the NQR end of the continuum, the transitions are all perturbed to first order by the magnetic field, but for NMR, at least the central transition is only perturbed to second order. Perhaps this sheds some light on the observation of ^{35}Cl NMR at 11.7 T for NaClO_3 .^[11] In this case, the quadrupole and the Zeeman interaction are both strong and of comparable magnitude. A plot of the calculated transition frequencies as a function of magnetic field^[11] shows that at this stage, NMR-like behavior is well-established. Perhaps spins prefer NMR.

Reference

- [1] M. H. Cohen, F. Reif. *Solid State Physics* **1957**, 5, 321–438.
- [2] G. M. Volkoff. *Can. J. Phys.* **1953**, 31, 820–836.
- [3] M. E. Smith, E. R. H. van Eck. *Prog. Nucl. Magn. Reson. Spectrosc.* **1999**, 34, 159–201.
- [4] A. Jerschow. *Prog. Nucl. Magn. Reson. Spectrosc.* **2005**, 46, 63–78.
- [5] R. E. Wasylishen, S. Wimperis, S. E. Ashbrook, *NMR of Quadrupolar Nuclei in Solid Materials*, Wiley, New York, **2012**.
- [6] T. P. Das, E. L. Hahn, *Nuclear Quadrupole Resonance Spectroscopy*, Academic Press, New York, **1958**.
- [7] M. Bloom, E. L. Hahn, B. Herzog. *Phys. Rev.* **1955**, 97, 1699–1709.
- [8] C. M. Widdifield, A. D. Bain, D. L. Bryce. *Phys. Chem. Chem. Phys.* **2011**, 13, 12413–12420.
- [9] F. A. Perras, C. M. Widdifield, D. L. Bryce. *Solid State Nucl. Magn. Reson.* **2012**, 45–46, 36–44.
- [10] H. Zeldes, R. Livingston. *J. Chem. Phys.* **1957**, 26, 1102–1106.
- [11] M. Khasawneh, J. S. Hartman, A. D. Bain. *Mol. Phys.* **2004**, 102, 975–983.
- [12] E. A. Donley, J. L. Long, T. C. Liebisch, E. R. Hodby, T. A. Fisher, J. Kitching. *Phys. Rev. A* **2009**, 79, 013420.
- [13] P. T. Eles, C. A. Michal. *Chem. Phys. Lett.* **2003**, 376, 268–273.
- [14] P. T. Eles, C. A. Michal. *Prog. Nucl. Magn. Reson. Spectrosc.* **2010**, 56, 232–246.
- [15] M. J. Weber, E. L. Hahn. *Phys. Rev.* **1960**, 120, 365–375.
- [16] J. B. Miller, B. H. Suits, A. N. Garroway. *J. Magn. Reson.* **2001**, 151, 228–234.
- [17] Y. K. Lee, H. Robert, D. K. Lathrop. *J. Magn. Reson.* **2001**, 148, 355–362.
- [18] D. Possa, A. C. Gaudio, J. C. C. Freitas. *J. Magn. Reson.* **2011**, 209, 250–260.
- [19] C. N. Banwell, H. Primas. *Mol. Phys.* **1963**, 6, 225–256.
- [20] J. Jeener. *Adv. Magn. Res.* **1982**, 10, 1–51.
- [21] A. D. Bain, B. Berno. *Prog. Nucl. Magn. Reson. Spectrosc.* **2011**, 59, 223–244.
- [22] H. J. Stoeckmann, D. Dubbers. *New J. Phys.* **2014**, 16, 053050.
- [23] R. R. Ernst, G. Bodenhausen, A. Wokaun, *Principles of Nuclear Magnetic Resonance in One and Two Dimensions*, Clarendon Press, Oxford, **1987**.
- [24] M. Mehring, *Principles of High Resolution NMR in Solids*, Springer-Verlag, Berlin, **1983**.
- [25] G. J. Bowden, W. D. Hutchison. *J. Magn. Reson.* **1986**, 67, 403–414.
- [26] G. J. Bowden, W. D. Hutchison, J. Khachan. *J. Magn. Reson.* **1986**, 67, 415–437.
- [27] B. C. Sanctuary. *J. Chem. Phys.* **1976**, 64, 4352–4361.
- [28] B. C. Sanctuary, T. K. Halstead. *Adv. Magn. Opt. Reson.* **1990**, 15, 79–161.

- [29] J. D. van Beek, M. Carravetta, G. C. Antonioli, M. H. Levitt. *J. Chem. Phys.* **2005**, *122*, 244510.
- [30] S. Vega. *J. Chem. Phys.* **1978**, *68*, 5518–5527.
- [31] D. M. Brink, G. R. Satchler, *Angular Momentum*, Oxford University Press, Oxford, **1968**.
- [32] R. N. Zare, *Angular Momentum: Understanding Spatial Aspects in Chemistry and Physics*, John Wiley & Sons, New York, **1988**.
- [33] A. D. Bain. *Mol. Phys.* **2003**, *101*, 3163–3175.
- [34] D. I. Hoult, C. N. Chen, V. J. Sank. *Magn. Reson. Med.* **2015**, *1*, 354–360.
- [35] E. Fukushima, S. B. W. Roeder, *Experimental Pulse NMR. A Nuts and Bolts Approach*, Addison-Wesley, Reading, Mass., **1981**.
- [36] K. J. Packer, K. M. Wright. *Mol. Phys.* **1983**, *50*, 797–813.
- [37] O. W. Sorensen, G. W. Eich, M. H. Levitt, G. Bodenhausen, R. R. Ernst. *Prog. Nucl. Magn. Reson. Spectrosc.* **1983**, *16*, 163–192.
- [38] J. Keeler, *Understanding NMR Spectroscopy*, John Wiley and Sons, New York, **2005**.
- [39] P. C. Taylor, J. F. Baugher, H. M. Kriz. *Chem. Rev.* **1975**, *75*, 203–240.
- [40] A. D. Bain. *Concepts Magn. Reson.* **2013**, *42*, 45–58.
- [41] A. D. Bain. *J. Magn. Reson.* **2006**, *179*, 308–310.
- [42] G. S. Harbison, A. Slokenbergs, T. M. Barbara. *J. Chem. Phys.* **1989**, *90*, 5292–5298.
- [43] A. D. Bain. *Prog. Nucl. Magn. Reson. Spectrosc.* **1988**, *20*, 295–315.
- [44] J. H. Wilkinson, *The Algebraic Eigenvalue Problem*, Clarendon Press, Oxford, **1965**.
- [45] G. H. Golub, C. F. van Loan, *Matrix Computations*, Johns Hopkins University Press, Baltimore, **1996**.
- [46] D. R. Muhandiram, R. E. D. McClung. *J. Magn. Reson.* **1987**, *71*, 187–192.
- [47] A. D. Bain. *Prog. Nucl. Magn. Reson. Spectrosc.* **2003**, *43*, 63–103.
- [48] A. D. Bain, J. S. Martin. *J. Magn. Reson.* **1978**, *29*, 125–135.
- [49] L. E. Kay, R. E. D. McClung. *J. Magn. Reson.* **1988**, *77*, 258–273.
- [50] A. D. Bain. *Chem. Phys. Lett.* **2012**, *531*, 267–271.